Chiang Mai J. Sci. 2016; 43(1) : 206-214
http://epg.science.cmu.ac.th/ejournal/
Contributed Paper

Microstructure and Mechanical Properties of As-cast and Heat-treated 935AgCuBeSn Alloys

Siriwan Sakultanchareonchai [a], Torranin Chairuangsri [b] and Ekasit Nisaratanaporn*[a]

[a] Innovative Metals Research Unit, Department of Metallurgical Engineering, Chulalongkorn University, Bangkok, 10330, Thailand.

[b] Department of Industrial Chemistry, Faculty of Science, Chiang Mai University, Chiang Mai, 50200, Thailand.

*Author for correspondence; e-mail: ekasit.n@chula.ac.th

Received: 30 September 2014
Accepted: 27 November 2014

ABSTRACT

Microstructure and mechanical properties of as-cast and heat-treated 935AgCuBeSn alloys were studied. The alloys were cast by lost-wax process in a vacuum inductive furnace. Their chemical composition was determined by inductively-coupled plasma-optical emission spectroscopy. Conventional heat treatment processes of standard Sterling silver alloys were applied *viz.* holding time in ceramic flash before quenching for 15 min, homogenization at 750 °C for 60 min followed by water quenching, and aging at 350 °C for 15 to 60 min followed by water quenching. Microstructural characterization was carried out by scanning electron microscopy and transmission electron microscopy to study the overall microstructure and precipitates formed by age hardening. It was found that homogenization treatment resulted in partial dissolution and spheroidization of eutectic phases, including α-Ag, β-Cu and a Cu-rich phase containing Ag and Sn, without significant grain coarsening. Aging treatment led to precipitation of fine fcc (Cu,Sn)-rich precipitates. This precipitation led to an improvement in hardness, yield strength and the modulus of resilience of the age-hardened 935AgCuBeSn alloys as compared to those of the conventional 935AgCu alloy.

Keywords: silver alloys, sterling silver, heat treatment, age hardening, microstructure, mechanical properties, electron microscopy

1. INTRODUCTION

Standard Sterling silver alloys contain copper as a major alloying element and their silver content is typically 92.5wt% Ag - so called 925AgCu alloys or 925 Sterling silver alloys [1]. These alloys can be strengthened by aging treatment similar to common heat treatable metals [e.g. 2,3]. The usual heat treatment processes for binary 925AgCu alloys are homogenization treatment above 745 °C to dissolve all the copper in the silver matrix, rapid quenching in cold water to prevent formation of coarse Cu-rich precipitates and to create super-saturated state, and aging at low temperature leading to a formation of very fine Cu-rich precipitates [1]. Even though some improvement of alloy properties can

be achieved by such conventional 925AgCu alloys and heat treatment processes, further development is still essential in some specific applications, e.g. spring parts in new jewelry products, where a higher content of silver at 93.5wt%Ag (so called 935AgCu alloys) is required for a better resistance to fire staining and tarnishing.

Even though many additional alloying elements in Ag-Cu alloys (e.g. Al, Au, Ge, Ir, Mn, Pd, Pt, Se, Te and Zn) have been studied in previous works [1, 4-7], the objectives of investigation were towards solving problems in porosity, fire staining, tarnishing or grain refining to compensate effects of broad melting range and heat treatments. Regarding mechanical properties of Sterling silver, Cu increases hardness in the as-cast state, allows age hardening by heat treatment, and increases strengthening effects during work hardening [1]. Cd [8] reduces the oxygen content in sterling silver and has a detrimental effect on strength. Ge has similar effects on anti-tarnishing of sterling silver as Al, but ductility is reduced at 7.5wt%Ge addition [9]. Nisaratanaporn *et al.* [6] reported the positive effect of Mn addition on Sterling silver alloys. The recommended Mn content in Sterling silver alloys for good tarnish and general corrosion resistance is 1-3wt%, with acceptable decreasing in hardness and strength of Sterling silver alloys due to decreasing of Cu content. It was found that eutectic structure, and therefore tensile strength, yield strength and hardness of the alloys, decreased as the Mn content was increased. Si has a detrimental effect on tensile strength and elongation due to promoting of large grain size [10]. An increase in Si or Ca added for anti-tarnishing of Sterling silver alloys led to a decrease in eutectic structure and hence strength and hardness of the alloys [1]. Zn (up to 4.5wt%) significantly reduced the porosity of the as-cast structure of 925AgCuZn alloy, induced grain coarsening during intermediate annealing, and led to a decrease of solution-annealed hardness and aged hardness [11]. Zn reduces the oxygen content in Sterling silver alloys and, together with Si, helps to avoid fire staining, but has a detrimental effect on strength [7].

Be and Sn are among alloying elements with a potential for precipitation hardening in Sterling silver alloys [5]. Silver alloys containing a minimum of 90wt%Ag with up to 1.5wt% Be have been invented [12,13] exhibiting resistance to tarnishing superior to that of the corresponding alloys without Be. Recently, microstructure and resiliency of 935AgCuBe alloys without Sn addition were studied [14] and promising properties were reported. Therefore, in the present work, microstructure and mechanical properties of 935AgCuBeSn alloys in as-cast and heat-treated conditions were investigated to understand effects of Be and Sn in precipitation hardening and mechanical properties of 935AgCuBeSn alloys. It was found that precipitation hardening can be accelerated by addition of Be and Sn as compared to that of the corresponding 935 AgCu alloy without Be and Sn addition. Aging treatment can be performed at 350 °C for a relatively short time of 30 min to form fine dispersion of fcc (Cu,Sn)-rich precipitates and to obtain an improvement in hardness, yield strength and the modulus of resilience of the 935AgCuBeSn alloys.

2. MATERIALS AND METHODS

2.1 Materials

The studied alloys were cast by lost-wax process at a pouring temperature of 1050 °C using a vacuum inductive furnace and ceramic plaster molds heated at 550 °C. High purity silver (99.99 wt%Ag), tin (99.9 wt%Sn) and a copper alloy (90wt%Cu-10wt%Be) were used as raw materials for preparing experimental

alloys with chemical composition, determined by inductively-coupled plasma - optical emission spectroscopy (ICP-OES), as given in Table 1. The chemical composition reported was averaged from three measurements. The reference alloy (R) is the corresponding 935 AgCu without addition of Be or Sn to compare mechanical properties, whereas the A1 and A2 alloys are 935 AgCuBeSn with an increment of Sn content.

Table 1. Chemical composition of experimental alloys determined by ICP-OES.

Alloy	wt%						
	Cu		Be		Sn		Ag
	Mean	STD*	Mean	STD*	Mean	STD*	
R	6.47	0.063	-	-	-	-	Bal.
A1	5.85	0.025	0.21	0.012	0.17	0.013	Bal.
A2	6.05	0.031	0.25	0.009	0.35	0.008	Bal.

* STD = standard deviation

2.2 Heat Treatments

Conventional heat treatment processes for age hardening of standard Sterling silver alloys were applied [1]. Holding time in ceramic flash before quenching was 15 min. This is within the optimum time range for effective homogenization during casting without precipitation of coarse copper particles in the silver matrix [1]. Quenching was performed in water at room temperature. Homogenization treatment was carried out at 750 °C for 60 min followed by water quenching. Aging treatment was performed at 350 °C for 15 to 60 min followed by water quenching.

2.3 Microstructural Characterization

Cylindrical specimens (9 mm in diameter and 4 mm in thickness) for scanning electron microscopy (SEM) to study the overall microstructure were ground by SiC paper down to 2000 grids and polished by diamond pastes down to □ μm. A JEOL JSM-6400 LV scanning electron microscope, equipped with an energy-dispersive X-ray spectrometry (EDS) detector (Inca, Oxford Instrument) was utilized and operated at 20 kV. The volume percentage of eutectic phases was determined from area fraction in SEM images using the ImageJ software. When etched by a solution containing 50 vol%NH_4OH, 25 vol%H_2O_2 and 25 vol%H_2O, grain boundaries can be revealed so that grain size can be estimated by the mean linear intercept method [15].

Specimens for transmission electron microscopy (TEM) to study precipitates after age hardening were cut as thin slices about 250 μm in thickness using a high precision cutting machine (Struers, Accutom 5) and SiC wheels. The slices were ground to reduce thickness down to 50-70 μm by 1200-grid SiC paper. Discs with 3 mm in diameter were then punched out. Twin-jet electropolishing (Struers, Tenupol III) was utilized to prepare thin foils for TEM, using a solution of 10 w/v% KCN in distilled water as electrolyte, and operated at 10 V and 25 °C. A JEOL, JEM-2010 scanning-transmission electron microscope was used and operated at 200 kV with EDS detector (Inca, Oxford Instrument). Crystallographic information of precipitates was interpreted from selected-area electron diffraction patterns (SADPs), whereas their chemical composition was obtained from EDS spectra.

2.4 Mechanical Properties

Specimens prepared for SEM were also used for hardness measurement using a Galileo Microscan OD V.98 hardness tester and 10 gf load ($HV_{0.01}$) at 15-seconds indentation time. The mean value was based on five different areas.

Yield strength and elongation of the experimental alloys were measured following the ASTM E8-96. A Lloyd universal testing machine with the maximum load of 10kN was utilized and the tensile test was performed at 0.75 mm/minute. The modulus of resilience (U_r), which relates to spring properties and is defined as the storage energy per unit volume in elastic-deformation range, was determined from the following the equation:

$$U_r = \frac{\sigma_y^2}{2E} \quad (1)$$

where σ_y is the yield strength and E is the Young modulus [16]. The values are average from 3 tensile-test bars.

3. RESULTS AND DISCUSSION

3.1 Overall Microstructure

Figures 1 to 3 compare the overall microstructure of the R, A1 and A2 alloys from SEM in the as-cast and different heat treatment conditions. Eutectic phases found in the reference alloy include eutectic α-Ag and β-Cu, whereas a Cu-rich phase containing Ag and Sn was additionally found in the A1 and A2 alloys containing Be and Sn (for example as shown in Figure 4). The amount of these eutectic phases decreased in the 935 AgCuBeSn alloys (as shown in Table 2) due possibly to a decrease in the copper content. The eutectic phases are partly dissolved by homogenization treatment, but aging treatment had negligible effect on dissolution of these phases. Grain size of all studied alloys as estimated from the mean linear intercept is comparable in the range of 200-300 μm and grain coarsening was not observed after homogenization treatment, implying that grain boundaries are effectively pinned by the remaining eutectic or Cu-rich phases. Spheroidization of the eutectic phases was noticeable after homogenization. However, precipitates formed by aging treatment in the silver matrix cannot be revealed by SEM.

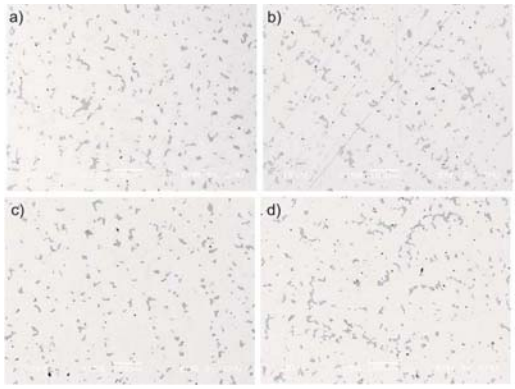

Figure 1. Backscattered electron images from SEM show the overall microstructure of the reference (R) alloy: (a) As-cast, 15 min holding time in flash, (b) 15 min holding time in flash+homogenization, (c) 15 min holding time in flash+homogenization + 30 min aging, and (d) 15 min holding time in flash+homogenization+60 min aging.

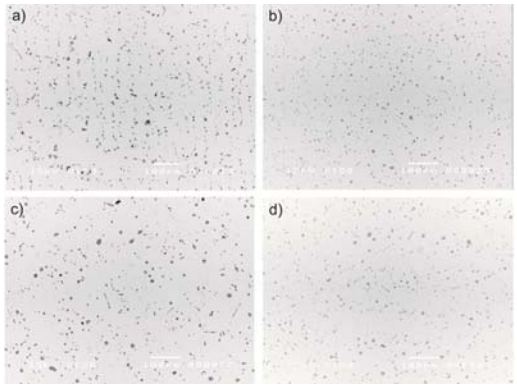

Figure 2. Backscattered electron images from SEM show the overall microstructure of the A1 alloy: (a) As-cast, 15 min holding time in

flash, (b) 15 min holding time in flash+homogenization, (c) 15 min holding time in flash+homogenization + 30 min aging, and (d) 15 min holding time in flash+homogenization+60 min aging.

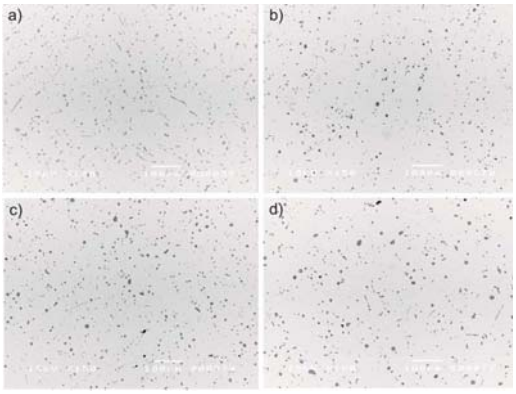

Figure 3. Backscattered electron images from SEM show the overall microstructure of the A2 alloy: (a) As-cast, 15 min holding time in flash, (b) 15 min holding time in flash+homogenization, (c) 15 min holding time in flash+homogenization + 30 min aging, and (d) 15 min holding time in flash+homogenization+60 min aging.

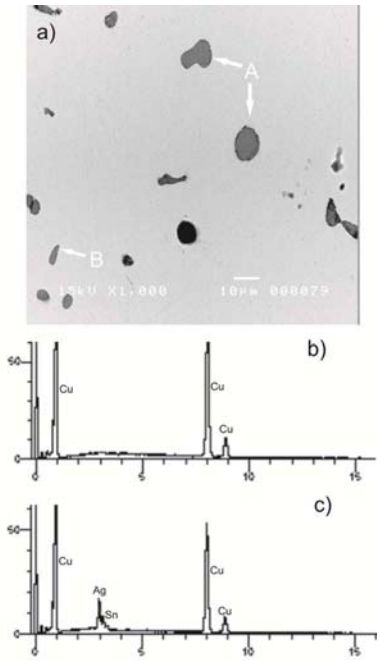

Figure 4. (a) Backscattered electron image from SEM of the A1 alloy (15 min holding time in flash+homogenization+30 min aging at 350 °C). (b) SEM-EDS spectrum from eutectic β-Cu (marked 'A'). (c) SEM-EDS spectrum from a Cu-rich phase containing Ag and Sn (marked 'B').

Table 2. Volume percentage of eutectic phases in the experimental alloys in the as-cast and heat-treated conditions.

Alloy	Volume Percentage of Eutectic Phases				
	As-cast	Homogenization	Homogenization + 15-min aging	Homogenization + 30-min aging	Homogenization + 60-min aging
R	5.45	4.15	4.13	4.14	4.14
A1	3.66	3.37	3.21	3.23	3.25
A2	3.73	2.62	2.74	2.76	2.76

3.2 Aging Precipitation

Aging precipitation in the 935 AgCuBeSn alloys can be represent by the results from TEM observation given in Figures 5 and 6. Figure 5 shows a bright-field (BF) TEM micrograph demonstrating an α-Ag dendrite in the as-cast A2 alloy, when the incident electron beam is parallel to $[01\bar{1}]_{fcc\ \alpha\text{-}Ag}$ as seen from corresponding SADP. No precipitate was observed in this condition.

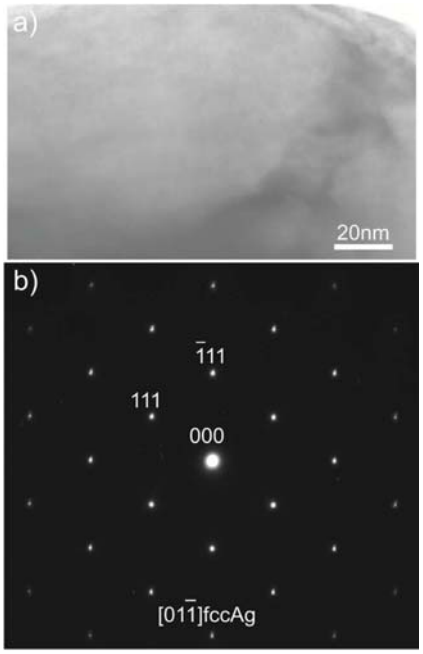

Figure 5. (a) BF-TEM micrograph of the A2 alloy in the as-cast condition. (b) corresponding SADP from $[01\bar{1}]_{fcc\ \alpha\text{-}Ag}$.

Figure 6 shows a BF-TEM micrograph of the A1 alloy after aging for 30 min. The incident electron beam is also parallel to as seen from the corresponding SADP. Fine precipitates, apparently disc-shape with 3-20 nm in size, were observed dispersing in the α-Ag matrix. The results from TEM-EDS revealed high content of Cu and Sn in the precipitates. Interpretation of SADPs revealed that the precipitates have a structure closed to fcc α-(Cu,Sn) according to JCPDS file No. 44-1477, a = 3.655 Å, Space Group = Fmm (225) [17]. Strain-field contrast was observed, so that coherency between the matrix and the precipitates can be presumed. A cube-cube orientation relationship was found between the precepitates and the α-Ag matrix, e.g. in Figure 6(b). This orientation relationship led to parallel Moiré fringes from $g[020]_{(Cu,Sn)}//g[020]_{\alpha\text{-}Ag}$ in Figure 5(a). The parallel distance of the fringes can be calculated from the equation: $(d_{[020](Cu,Sn)}.d_{[020]\alpha\text{-}Ag})/ = (1.82x\times2.05)/(2.05\text{-}1.82) = 16.2$, which is fairly close to that measured from the BF-TEM image. Due to limitation of TEM-EDS detector, the content of Be has not been known and the possible formation of phases containing a combination of Cu, Be and Ag cannot be neglected. Fcc Cu-rich precipitates with a cube-cube orientation relationship to the fcc α-Ag matrix leading to parallel Moiré fringes has been found in the 935AgCuBe alloy after ageing at 300 °C for 60 min [14]. In the present study, Be and Sn addition to the 935AgCu alloys led to an acceleration in precipitation hardening, so that a relatively shorter aging time of 15-30 min at 350 °C can be applied for a comparable distribution of precipitates.

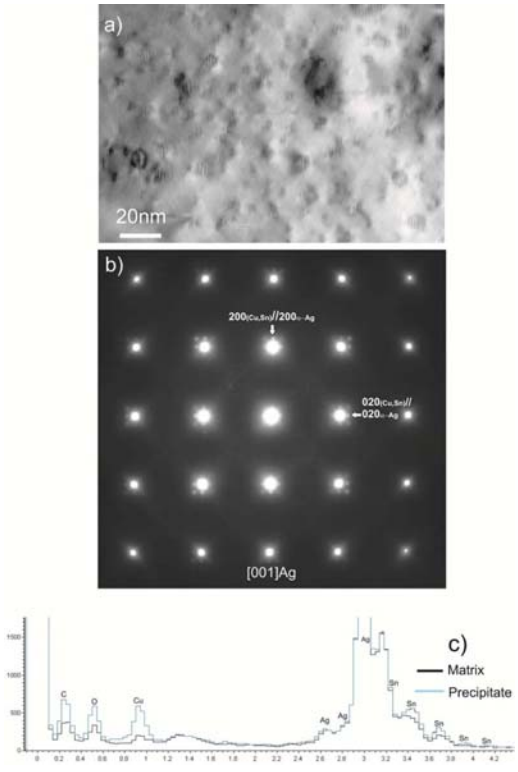

Figure 6. (a) BF-TEM micrograph of the A1 alloy after aging treatment at 350 °C for 30 min, (b) Corresponding SADPs from zone $[001]_{fcc\ \alpha\text{-}Ag}$ showing a cube-cube orientation relationship, and (c) EDS spectra from a precipitate and the Ag matrix.

3.3 Mechanical Properties

Hardness, yield strength, elongation and the modulus of resilience of the experimental alloys are given in Tables 3 to 6. Aging treatment led to an increase of the alloy hardness and the effect of Be and Sn on increasing of the alloy hardness was significant in the A2 alloy with about 0.4 wt%Sn addition. Additions of Be and Sn in the range used in this experiment led to an improvement of yield strength and the modulus of resilience in the age-hardened alloys. These can be attributed to precipitation of fine (Cu,Sn)-rich precipitates as observed in TEM. Even though the highest yield strength and the modulus of resilience were obtained from the A2 alloy with a higher Sn content and at a prolonged aging time of 60 min, the A1 alloys with a lower Sn content and a shorter aging time of 30 min was considered to be appropriate for practical point of view in jewelry applications. Moreover, it should be noted that a decrease in elongation of the 935 AgCuBeSn alloys will not be the problem in practice, because heat treatments are usually preformed after product assembling. Thus, the values of elongation shown in Table 5 were sufficient for jewerly usage.

Table 3. Hardness of the experimental alloys in the as-cast and heat-treated conditions.

Alloy	Hardness($HV_{0.01}$)				
	As-cast	Homogenization	Homogenization + 15-min aging	Homogenization + 30-min aging	Homogenization + 60-min aging
R	61±7	59±4	130±2	123±3	123±1
A1	59±3	63±4	84±8	113±2	116±7
A2	60±2	59±3	143±3	137±2	158±2

Table 4. Yield strength of the experimental alloys in the as-cast and heat-treated conditions.

Alloy	Yield Strength (MPa)				
	As-cast	Homogenization	Homogenization + 15-min aging	Homogenization + 30-min aging	Homogenization + 60-min aging
R	78±4.9	74±6.4	84±7.1	88±9.9	123±8.5
A1	28±4.3	66±4.5	86±4.7	151±3.2	151±10.7
A2	51±2.0	64±0.7	160±3.8	173±11.3	217±4.3

Table 5. Elongation of the experimental alloys in the as-cast and heat-treated conditions.

Alloy	Elongation (%)				
	As-cast	Homogenization	Homogenization + 15-min aging	Homogenization + 30-min aging	Homogenization + 60-min aging
R	37.3±2.4	45.0±3.4	40.2±2.8	35.5±7.0	31.2±5.2
A1	26.1±2.9	7.7±0.5	3.4±0.3	7.2±0.7	8.3±3.3
A2	30.0±0.7	26.5±4.3	11.3±4.3	10.0±2.0	7.1±0.2

Table 6. Modulus of resilience of the experimental alloys in the as-cast and heat-treated conditions.

Alloy	Elongation (%)				
	As-cast	Homogenization	Homogenization + 15-min aging	Homogenization + 30-min aging	Homogenization + 60-min aging
R	0.49±0.12	0.43±0.32	0.55±0.18	0.63±0.06	1.07±0.28
A1	0.12±0.06	0.47±0.46	0.54±0.09	0.84±0.34	1.17±1.60
A2	0.22±0.02	0.31±0.07	1.20±0.15	1.15±0.30	1.75±0.32

4. CONCLUSIONS

Microstructure and mechanical properties of as-cast (15-min holding time in the ceramic flash) and heat-treated 935AgCuBeSn alloys were investigated. Homogenization treatment at 750 °C for 60 min resulted in partial dissolution and spheroidization of eutectic phases without significant grain coarsening. Aging treatment at 350 °C resulted in precipitation of fcc (Cu,Sn)-rich precipitates. This precipitation led an improvement in hardness, yield strength and the modulus of resilience of the age-hardened 935AgCuBeSn alloy as compared to those of the conventional 935AgCu alloy. The alloy with about 0.2wt%Be and 0.2wt%Sn additions and the aging time of 30 min at 350 °C were considered to be appropriate for practical point of view in jewelry applications.

ACKNOWLEDGEMENTS

The authors wish to acknowledge the financial and facility support by the Oldmoon Co., Ltd., the Thailand Research Fund (TRF), the National Research University Project under Thailand's Office of the Higher Education Commission, and the Post-Doctoral Scholarship supported by the Rachadapisaek Sompote Fund, the Graduate School of Chulalongkorn University, Thailand.

REFERENCES

[1] Fischer-Bühner J., Bertoncello R., Basso A. and Poliero M., *The Santa Fe Symposium on Jewelry Manufacturing Technology*, May 2010; 227-242.

[2] Du Y.Y., Lu Y.P., Li T.J., Wang T.M. and Zhang G.L., *Mater. Res. Innovations*, 2011; **15(2)**: 107-111, DOI 10.1179/143307511X 12998222918796.

[3] Amenova A., Belov N., Smagulov D. and Toleuova A., *Mater. Res. Innovations*, 2014; **18(S1)**: S50-S53, DOI 10.1179/1432891713Z.000000000350.

[4] Gardam G.E., *Metallurgia*, 1953; **47(279)**: 29-33.

[5] Strauss J.T., *The Santa Fe Symposium on Jewelry Manufacturing Technology*, May 2008; 307-326.

[6] Nisaratanaporn E., Wongsriruksa S., Pongsukitwat S. and Lothongkum G., *Mater. Sci. Eng. A*, 2007; 445-446: 663-668 DOI 10.1016/j.msea. 2006.09.106.

[7] Qingqing Y., Weihao X., Zhen Y., Dingjie S. and Ronghui W., *Rare Met. Mater. Eng.*, 2010; **39(4)**: 578-581, DOI 10.1016/S1875-5372(10)60092-6.

[8] Reti A.M., *The Santa Fe Symposium on Jewellery Manufacturing Technology*, 1997; 353-355.

[9] Johns P., *The Santa Fe Symposium on Jewellery Manufacturing Technology*, 1997; 38-42.

[10] Mccloskey J.C., Welch P.R. and Aithal S., *Gold Technol.*, 2000; **30**: 4-7, DOI 10.1007/BF03214802.

[11] Qingqing Y., Weihao X., Dingjie S.,

Zheng Y. and Ronghui W., *Rare Met. Mater. Eng.*, 2008; **37(6)**: 947-951. DOI 10.1016/S1875-5372(09)60026-6.

[12] Sloman H.A., *United State Pat.*, *No.* 399 (1932).

[13] McFarland J.C. and Fort T., *United State Pat.*, *No.* 1,984 (1932).

[14] Chairuangsri T. and Nisaratanaporn E., *Chiang Mai. J. Sci.*, 2010; **37(2)**: 260-268.

[15] Pickering F.B., *The Basis of Quantitative Metallography, Institute of Metallurgical Technicians, Monograph No. 1*, The Chameleon Press Ltd., Wandsworth, London, 1975.

[16] Piersol A. and Paez T., *Engineering Properties of Metals; Harris's Shock and Vibration Handbook*, 6th Edn., McGraw-Hill, 2009; 34.1-34.4.

[17] X-ray Powder Diffraction File *JCPDS - ICDD* 2001 (Joint Committee on Powder Diffraction Standard International Centre for Diffraction Data, Swarthmore, PA) 44-1477.